PROCEEDINGS OF SCIENCE

PID performance in Run 2 at LHCb

Alex Seuthe[1,*]
Technische Universität Dortmund, Otto-Hahn-Straße 4, 44227 Dortmund, Germany
E-mail: alex.seuthe@cern.ch

The LHCb particle identification (PID) is crucial for LHCb flavour physics. The LHCb PID system consists of two ring-imaging Cherenkov detectors, a calorimeter system, and muon chambers. Information of those sub-detectors is combined in powerful PID observables using multivariate classifiers to achieve an optimum of separation quality. The detector's PID efficiencies are calculated with dedicated calibration data samples which are recorded with a new computing strategy in Run 2 of the LHC. The general PID strategy in Run 2 is presented as well as the PID performance for charged and neutral particle species as a key part of the LHCb physics programme.

The Eighth Annual Conference on Large Hadron Collider Physics-LHCP2020
25-30 May, 2020
online

[1]on behalf of the LHCb Collaboration.
*Speaker

https://pos.sissa.it/

PoS(LHCP2020)047

1. Particle Identification at LHCb

Particle Identification (PID) is a crucial part of LHCb's flavour physics programme. The dedicated PID system of the LHCb detector in Run 2 consists of different sub-systems: two ring-imaging Cherenkov (RICH) detectors, a calorimeter system, and five muon stations [1]. The PID information from the detector sub-systems is combined into powerful single observables for the charged PID with the following observables: the $\mathrm{DLL}_{X\pi}$ observable is the log-likelihood difference of particle hypotheses of the particle species X and pions as reference. The likelihood from each sub-system is multiplied to build the combined observables $\mathcal{L} = \mathcal{L}_{\mathrm{RICH}} \cdot \mathcal{L}_{\mathrm{Calo}} \cdot \mathcal{L}_{\mathrm{Muon}}$. The `ProbNNX` observables are calculated as the output of dedicated neural networks, trained on simulation with input from the detector components and tracking information. For the PID of neutral particle species separate neural networks are employed. Because simulation is not perfectly describing the PID response, a calibration with data-driven techniques and large calibration data samples is performed [2].

2. PID calibration samples

The PID calibration samples are selected in Run 2 as follows. Collision data is filtered with the LHCb trigger system consisting of the hardware trigger (L0) and the software-based high level triggers (HLT1 and HLT2). The selection of the calibration samples takes place at the HLT2 level with a dedicated trigger stream. This allows to save resources thanks to centralised computation, and to control systematic uncertainties in a consistent manner [3]. The calibration is performed using the tag-and-probe method with a tight selection on the tag particles and no PID requirements on probe particles. The calibration samples use decay modes with low multiplicity and large branching ratios to ensure high purity and large sample sizes. Tab. 1 shows decays used to extract the charged and neutral calibration samples and Fig. 1 presents the invariant mass distributions of the neutral calibration samples. The calibration samples are used to evaluate the PID efficiencies in the physics analyses. This is done by applying a given PID requirement on the relevant calibration sample and evaluating its efficiency as a function of kinematic observables of the track. This reduces systematic effects due to the mismodelling of the PID efficiencies in simulation.

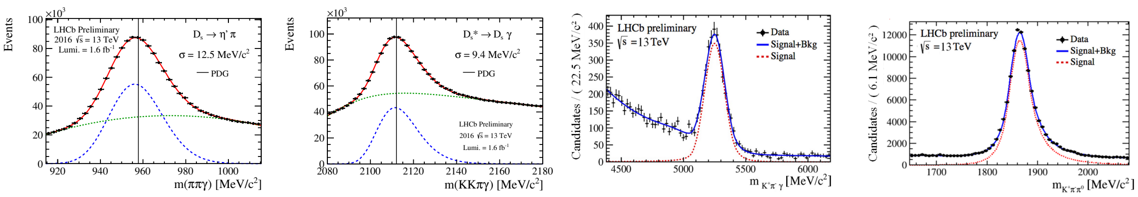

Figure 1: Invariant mass fits of candidates of the PID calibration samples for neutral particle species. For the photon PID the decays $D_s^+ \to [\rho^0\gamma]_{\eta'}\pi^+$, $D_s^* \to D_s^+\gamma$, and $B^0 \to K^{*0}\gamma$ are shown. For the neutral pion PID the decay $\overline{D}^0 \to K^+\pi^-\pi^0$ is shown. In the first two plots data is represented by black dots, the signal and background components by the blue and green dashed lines and the total distributions by the red curves. For the last two plots data is represented by black dots, the signal components by the red dotted lines, and the total distributions by the blue solid lines. [4]

Species	Low momentum	High momentum
$e^{\pm}$	$B^+ \to J/\psi\, K^+$ with $J/\psi \to e^+e^-$	
$\mu^{\pm}$	$B^+ \to J/\psi\, K^+$ with $J/\psi \to \mu^+\mu^-$	$J/\psi \to \mu^+\mu^-$
$\pi^{\pm}$	$K^0_S \to \pi^+\pi^-$	$D^{*+} \to D^0\pi^+$ with $D^0 \to K^-\pi^+$
$K^{\pm}$	$D_s^+ \to \phi\pi^+$ with $\phi \to K^+K^-$	$D^{*+} \to D^0\pi^+$ with $D^0 \to K^-\pi^+$
$p, \overline{p}$	$\Lambda \to p\pi^-$	$\Lambda \to p\pi^-$; $\Lambda_c \to pK^-\pi^+$
γ	$D_s^+ \to [\rho^0\gamma]_{\eta'}\pi^+$	$B^0 \to K^{*0}\gamma$
	$D_s^* \to D_s^+\gamma$	
π^0	$\overline{D}^0 \to K^+\pi^-\pi^0$	

Table 1: Decay modes employed to compute the PID calibration samples of charged particle species. To cover different phase space regions, different decay channels are used. Charge conjugate processes are included.

3. PID performance

The performance of the combined PID observables is assessed as the efficiency and misidentification rate for a given PID cut as a function over the particle species' momentum. Fig. 2 shows the performance for the `DLL` variable with a loose and a tight cut for muons, electrons, kaons, and protons and shows a very good discrimination power over wide kinematic ranges. As an example it can be seen in the PID performance for kaons that the efficiency to correctly identify a kaon is larger than 80 % up to a momentum of $p = 100$ GeV for a loose cut, while the pion misidentification rate is significantly reduced employing a tight cut. The muon, electron and proton performances show very high identification efficiencies with very small misidentification rates as well. For the neutral performance three different neural networks trained with Run 1 simulation to separate photon signatures from other species exist: The `IsNotH`, `IsNotE`, and `IsPhoton` observables are separating photons and hadrons, photons and electrons/positrons and photons and neutral pions, repectively. The response of the `IsNotH` and `IsNotE` classifiers can be seen in Fig. 2. New multivariate classifiers and calibration samples for deuteron PID are developed. Baryonic decays of the kind $\Lambda_b \to d\overline{p}$ or cross-section measurements of deuteron production are possible use cases. The `ProbNNd` distributions for charged tracks from simulation is shown in Fig. 2 where the deuteron candidates are extracted from simulated $\Lambda_b \to d\overline{p}$ decays and the other tracks from $\Lambda_c \to pK^-\pi^+$ decays.

4. Conclusion

With the dedicated PID system of the LHCb experiment an excellent PID performance is provided. Data-driven calibration methods allow to determine the PID efficiencies reducing the systematic effects due efficiency mismodelling in simulation. The PID separation power is shown for different particle species over a wide momentum range with high identification efficiencies and low misidentification rates as a key part of the LHCb physics programme.

PoS(LHCP2020)047

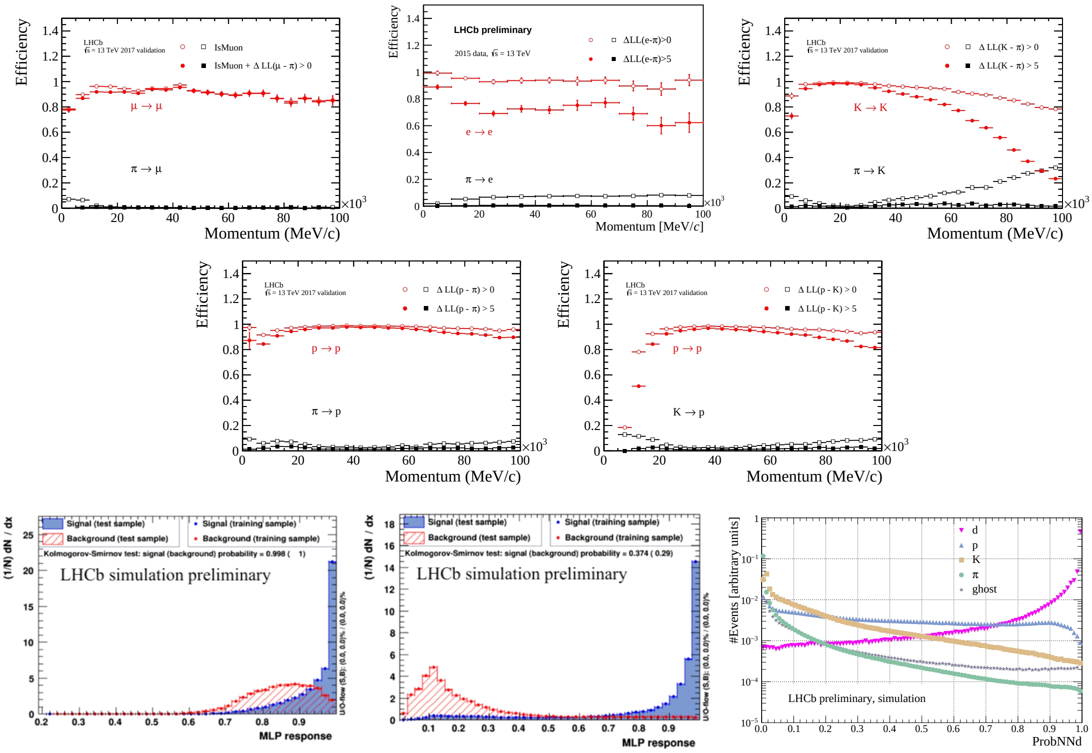

Figure 2: (Top and middle) efficiency and mis-identification probabilites for the charged PID DLL variables as a function of momentum for different species. [5]. (Bottom from left to right) Response of `isNotE` and `isNotH` classifiers with reconstructed photon candidates matching the generated photons (blue) and reconstructed photons matching generated electrons, and neutral pions (red), respectively [4] and response of the `ProbNNd` observable for deuterons [6].

References

[1] A. A. Alves et al. (LHCb Collaboration), *The LHCb Detector at the LHC*, *JINST* **3**, 8005 (2008).

[2] L. Anderlini et al. (LHCb Collaboration), *The PIDCalib package*, LHCb-PUB-2016-021, July 2016.

[3] R. Aaij et al. (LHCb Collaboration), *Selection and processing of calibration samples to measure the particle identification performance of the LHCb experiment in Run 2*, *EPJ Techn Instrum* **6**, 1 (2019).

[4] R. Aaij et al. (LHCb Collaboration), *Reconstruction, calibration, and PID performance for photons and neutral pions*, LHCB-FIGURE-2020-011, in preparation.

[5] R. Aaij et al. (LHCb Collaboration), *Global PID performance for charged particles*, LHCB-FIGURE-2020-012, May 2020.

[6] R. Aaij et al. (LHCb Collaboration), *Deuteron PID performance in LHCb simulation*, LHCB-FIGURE-2020-013, June 2020.